Cloud Heights and Nighttime Cloud Cover from TIROS Radiation Data

S. I. RASOOL

Goddard Institute for Space Studies, NASA, New York, N. Y.

(Manuscript received 15 November 1963)

ABSTRACT

Radiation data obtained from TIROS III have been analyzed, separately for day and for night, for the period July through September 1961. The global distribution of the average effective temperatures measured by the 8–12 μ channel of the satellite radiometer shows a close correlation with the cloud cover data.

An estimate of the latitudinal distribution of cloud heights has been obtained using the TIROS radiation data for daytime and the distribution of cloud cover recently obtained from the TIROS photographs. Combining these values of the cloud heights with the nighttime radiation data determines the latitudinal distribution of nighttime cloud cover.

The results indicate that in the Southern Hemisphere the percentage cloudiness at night is considerably higher than in the day, while in the case of the Northern Hemisphere the cloudiness appears to decrease at night.

1. Introduction

In a recent paper, Arking (1964) has derived the global distribution of cloud cover by the analysis of TIROS III video pictures. In Fig. 7 (Curve 1) is plotted the latitudinal distribution of average *daytime* percentage cloud cover as obtained by Arking for the period of 12 July through 10 September 1961.

In the present study we attempt, using these data and the simultaneous radiation measurements by TIROS III, to derive the average latitudinal distribution of *cloud top heights* and thence the *nighttime* cloud cover. Curve 2 in Fig. 7 shows the resulting percentage cloud cover during the night as a function of latitude.

2. TIROS infrared data

The radiation instrumentation in TIROS and the physical significance of this experiment have already been described by several authors (Bandeen *et al.*, 1961; Nordberg *et al.*, 1962). Three of the five channels of the TIROS radiometer measure terrestrial radiation in the far infrared corresponding to wavelength intervals of 5.8–6.5 μ, 8–12 μ, and 7–30 μ. The other two channels record the solar radiation in the visible, as reflected by the earth, to obtain an estimate of the albedo of any region. The wavelengths of the infrared channels have been chosen so as to provide information on the temperature at different levels of the atmosphere and to give an estimate of the total outgoing radiation in the infrared. In this discussion we shall only be concerned with Channel 2, sensitive in the 8–12 μ region of the infrared.

The main absorber of infrared radiation in the earth's atmosphere is water vapor. The absorption coefficient, however, varies considerably with wavelength between 4 and 50 μ, where almost all the energy of the terrestrial radiation is confined. In the 8–12 μ spectral interval the absorption by water vapor and also by CO_2, the other important absorber of the infrared radiation, is at its minimum. Consequently, *in the absence of clouds*, Channel 2 of the satellite radiometer, measuring in this atmospheric "window," records energy originating from very near the ground corresponding to an effective temperature only ~5–10 deg K less than the ground temperature (Wark, Yamamoto and Lienesch, 1962; Prabhakara and Rasool, 1963).

Reasonably thick clouds, however, are practically opaque to infrared radiation of wavelengths $>4\,\mu$ (Shiffrin, 1961). As there is very little water vapor above the clouds, and if we may assume that the albedo of the clouds in the far infrared is negligible, the radiometer *in the presence of thick clouds* will record energy corresponding to the cloud top temperature. This may be as much as 40–50 deg K lower than the surface temperature.

If, therefore, for any given instant, both the TIROS measured temperatures in this "window" channel and the actual surface temperatures are available, a knowledge of the temperature lapse rate in the atmosphere will enable one to obtain a quick estimate of cloud top height. On the other hand, on a climatological basis, if the satellite-measured temperatures for a given region are averaged over a season, then the departure of this temperature from the mean ground temperature will be mainly dependent on three variables—cloud amount, cloud height, and water vapor distribution in the atmosphere. As mentioned earlier, the effect of water vapor is comparatively small, and from our knowledge of climatological distribution of the water vapor over the

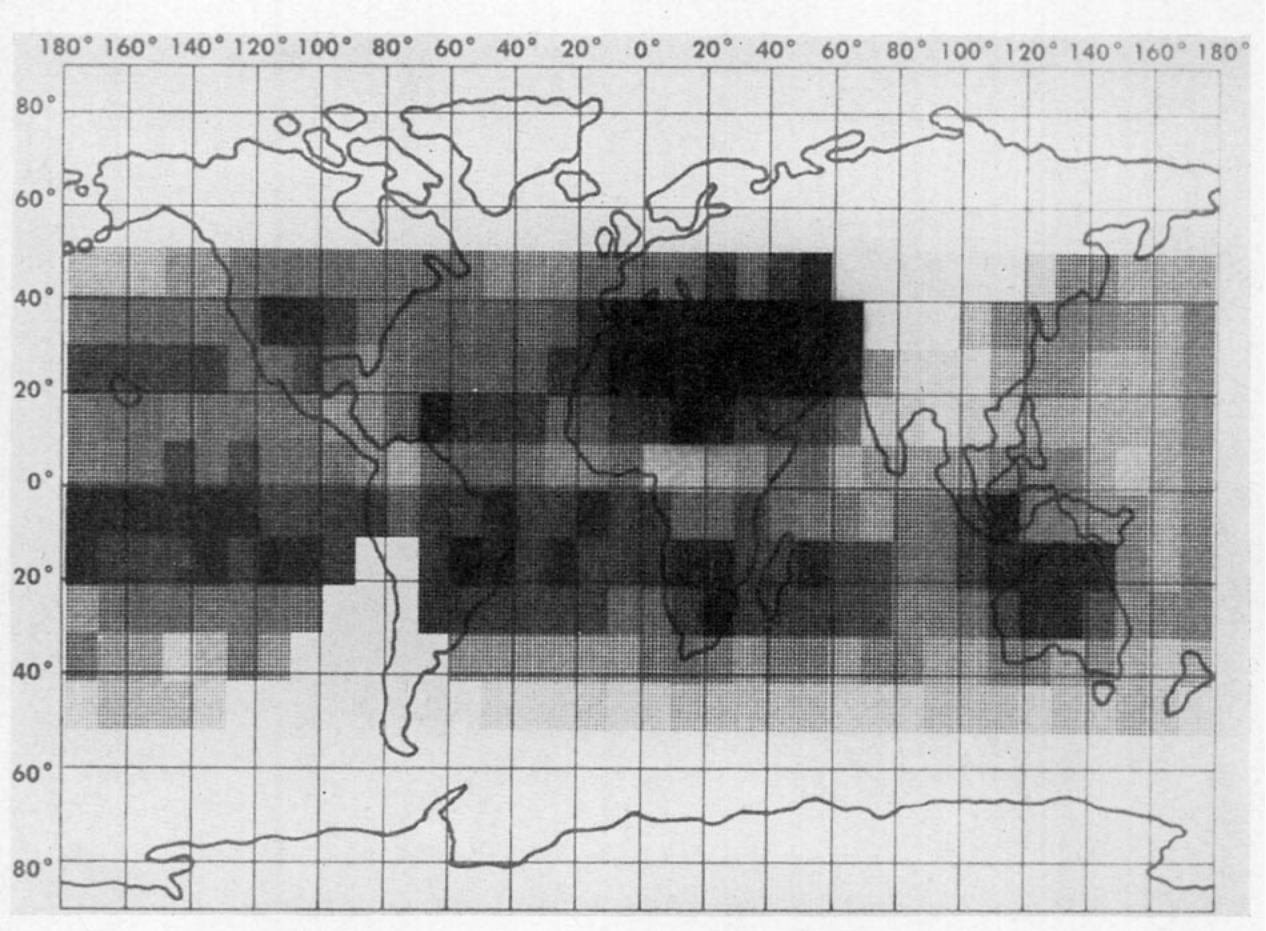

FIG. 1. Global distribution of average temperatures measured by TIROS radiometer Channel 2 for the period 12 July through 10 September 1961. Darkest shade, $T>295$K, lightest shade, $T<255$K.

globe, its effect on the temperatures measured by the satellite can be accounted for.

The strong effect of clouds on the TIROS III measured temperatures in the "window" channel is demonstrated by Fig. 1. In this figure are plotted the regional and temporal averages of the temperatures measured by Channel 2 of TIROS III during daytime (0600–1800 hours Local Time) for the period of July 12 through 10 September 1961. Measurements for the polar regions are not available because the inclination of the orbit was only about 48°. The surface of the earth between 50N and 50S has been divided into a 10 deg latitude by 10 deg longitude grid, and all measurements taken by the satellite in each grid at nadir angle <25 deg, between local time 0600 and 1800, have been averaged for this period. In most cases there are more than 500 observation points per grid. The observations were corrected for the instrumental degradation (Bandeen, private communication).

The very dark shades correspond to high radiation intensities with effective temperatures ranging above 290K. The lightest shades correspond to temperatures of the order of 240K. The two triangular areas, which are diagonally opposite and comprise a part of South America and Southern Siberia, have been left blank because of the unavailability of the telemetry from the TIROS for these regions.

Several interesting features are revealed by examining this figure. 1) The relatively cold temperature belt near the equator corresponds to the high cloudiness usually observed in the equatorial region. 2) The subtropical belt in each of the hemispheres show relatively higher temperatures and, therefore, probably fewer clouds than in the equatorial regions. 3) Extremely low temperatures measured over East Pakistan and India imply a heavy cloud cover over these regions which is, in all probability, the monsoon activity of this season. An almost quasipermanent cloud cover over central Africa is also indicated from this diagram.

These conclusions are supported by comparing Fig. 1 with Fig. 2 in which is plotted the global distribution of cloud cover, also in a 10×10 degree grid, taken from the climatological estimates of Haurwitz and Austin (1944). In Fig. 2, the darkest shades correspond to 20 per cent cloudiness, and the lightest to 70 per cent cloudiness. The agreement in the main features of the two figures is striking, except that the TIROS III measured extremely high temperatures over the South

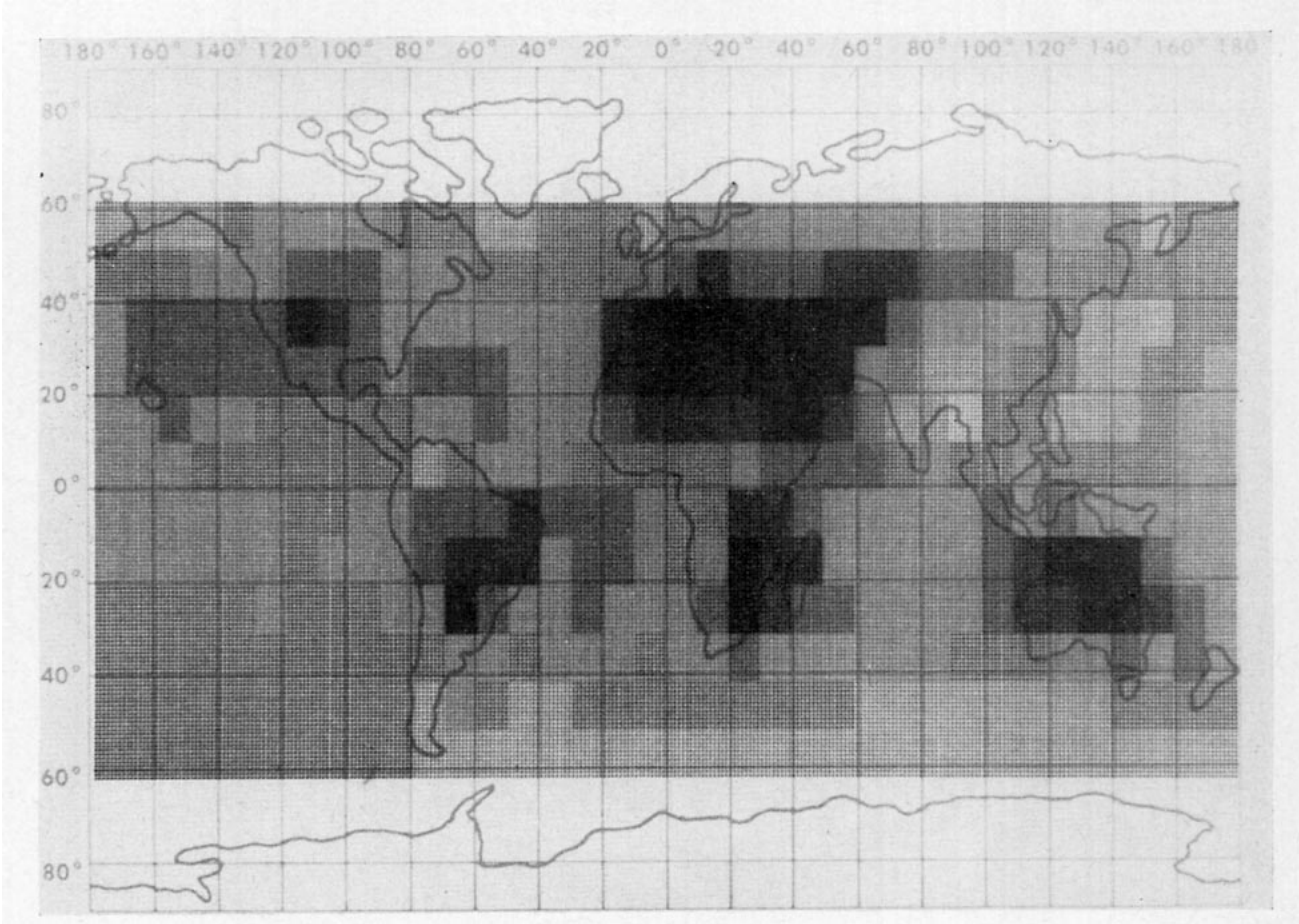

FIG. 2. Globa distribution of average cloud cover for July (after Haurwitz and Austin, 1944). Darkest shade—cloud cover <20 per cent, lightest shade—cloud cover >70 per cent.

Pacific, indicating a relatively clear area which is not noticeable in Fig. 2, undoubtedly due to lack of observational data in this region.

3. Deduction of cloud heights and cloud cover

Although it is interesting to note the resemblance between Figs. 1 and 2, the actual derivation of cloud amounts from the TIROS radiation data is fairly involved. As mentioned earlier, several factors, viz., cloud amount, cloud height, surface temperature, vertical distribution of water vapor and of temperature, influence the 'effective' temperatures measured by the satellite. By the method described below we have, however, attempted to separate the effect of these parameters in order to obtain a reasonable estimate of cloud height from TIROS radiation data.

Using the climatological estimates of the global distribution of surface temperature (Haurwitz and Austin, 1944), the latitudinal variations in the vertical distribution of temperature (Davis, 1962, London, 1957), the total amounts of water vapor and ozone and their vertical distributions, we have constructed ten different model atmospheres which correspond to the ten latitudinal belts between 50N and 50S for the months of July and August.

The radiation flux in the 8–12 μ region, which would be emitted from such atmospheres, was then calculated following a method described in an earlier paper (Prabhakara and Rasool, 1963). The flux values thus calculated give the equivalent black body temperatures TIROS will observe above these atmospheres *if the atmosphere were completely cloudless*. Similar calculations were then repeated assuming the presence of thick clouds at various altitudes and of varying proportions. It is assumed that the clouds are completely opaque to the far infrared and the radiation is emitted only from the top of the clouds.

In Figs. 3 and 4 the results obtained for two such model atmospheres are shown. The family of five curves shows the difference (ΔT) between the surface temperature and the effective black body temperature observed by the satellite in the presence of different amounts of clouds located at altitudes of 2, 3, 4, 5, or 6 km. The intersection point of these curves with the ordinate in Fig. 3 is at 11.5 deg. This indicates that in a hot and humid atmosphere, even in complete absence of clouds, the satellite would observe an effective temperature

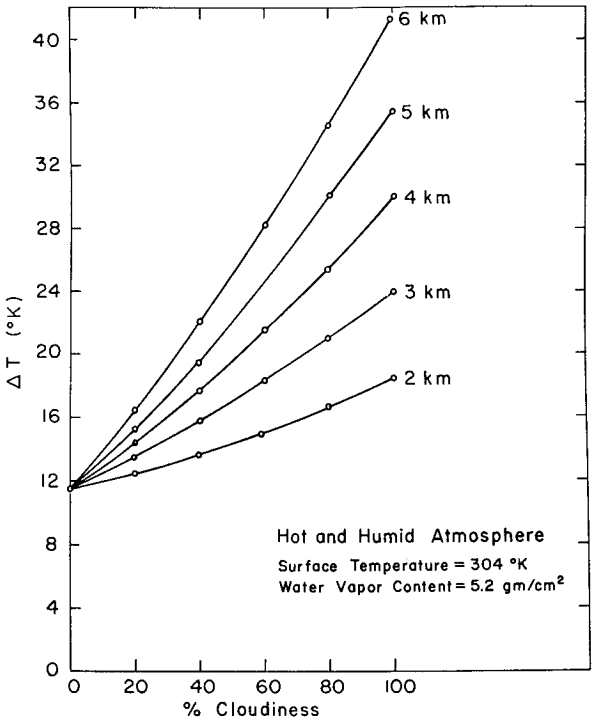

FIG. 3. ΔT as a function of percentage cloud cover with cloud tops at various altitudes. ΔT is the difference between the average surface temperature and the equivalent black body temperature measured by the TIROS III, Channel 2. A case of hot and humid atmosphere.

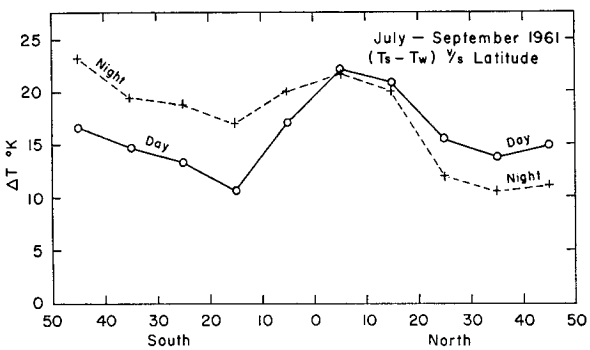

FIG. 5. ΔT as a function of latitude—for day and for night.

about 12 deg lower than the surface temperature. In Fig. 4 is shown another extreme case, this time of a dry and cold atmosphere where the ΔT, in the absence of clouds, is only 3.5 deg.

If, therefore, for any given region, one has an estimate of surface temperature, of the amount of water vapor in the atmosphere and of the percentage cloud cover, then with such a family of curves, combined with the TIROS radiation data of the "window" channel, one can derive an approximate value for the effective height of the cloud tops.

In order to determine the latitudinal distribution of the effective cloud heights for the months of July and

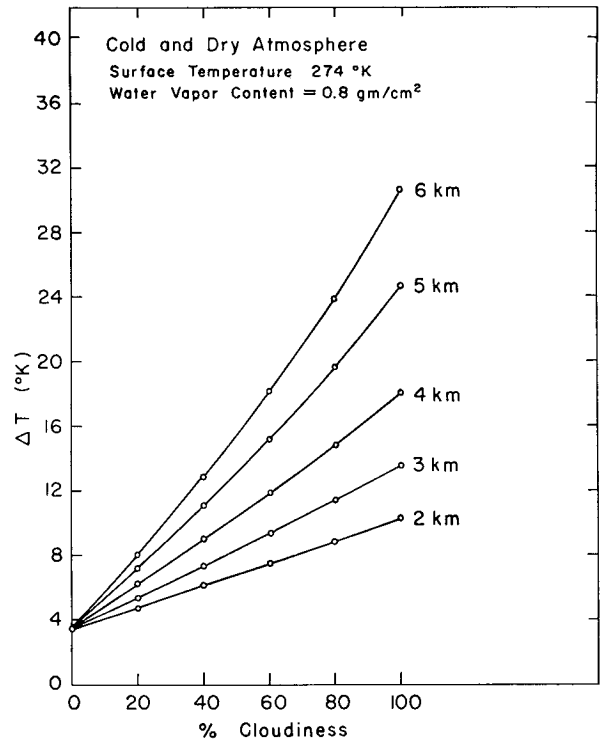

FIG. 4. Same as Fig. 3—a case of cold and dry atmosphere.

August 1961, we calculate the following parameters for each 10-deg latitudinal belt between 50N and 50S.

The satellite-observed temperatures in the "window" channel are averaged separately for day and for night for the period 12 July through 10 September 1961.

The latitudinal means of day and night surface temperatures for the same period were determined from the *Monthly Climatic Data of the World* (U. S. Weather Bureau); supplementing these data were climatological estimates of Haurwitz and Austin (1944) for the oceanic regions.

The difference (ΔT) between the mean surface temperatures and the average effective temperatures measured by the TIROS channel 2 in each latitudinal belt is plotted in Fig. 5 separately for day and for night.

Latitudinal averages of daytime percentage cloud cover for the same period given by Arking are shown in Fig. 7 (Curve 1).

Now with both the ΔT and percentage cloud cover being known for daytime, we can use our nomograms (e.g., Figs. 3 and 4) to determine the average daytime cloud height for each latitudinal belt. The heights thus deduced are plotted as a function of latitude in Fig. 6.

If we assume that, on an average, cloud heights derived from the daytime measurements are also valid for the night, we can now use the ΔT values for the night (Fig. 5) and the heights plotted in Fig. 6 to determine the nighttime cloud cover as a function of latitude.

The resulting latitudinal distribution of the nighttime cloud cover is plotted as Curve 2 in Fig. 7.

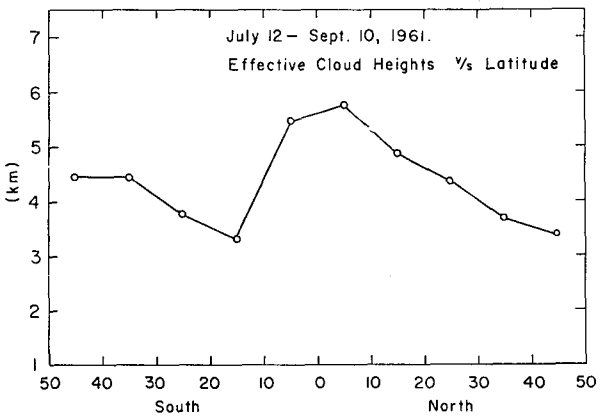

FIG. 6. Effective cloud top heights deduced from the daytime observation of TIROS III as a function of latitude.

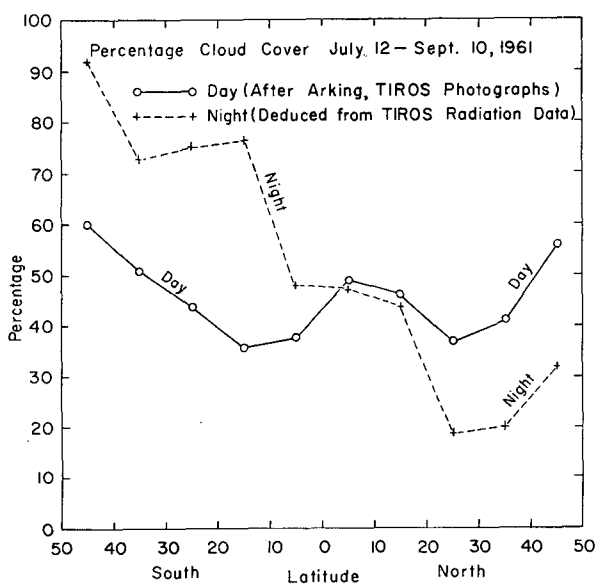

FIG. 7. *Curve 1.* Daytime average percentage cloud cover for the period 12 July through 10 September as a function of latitude (after Arking). *Curve 2.* Nighttime average percentage cloud cover for the same period deduced from TIROS window channel data.

A comparison of the day and night curves immediately shows that in the Southern Hemisphere, which is largely oceanic, the percentage cloudiness is much higher at night than during the day. In the Northern Hemisphere, on the other hand, the nocturnal cloud cover could be as low as ~20 per cent for the latitudes of 20 to 40 deg.

These results are based on the debatable assumption that, on an average, for a given latitudinal belt the cloud-top heights do not change from day to night. In case this assumption is not correct, our results would then indicate that, in order to have the same amount of cloudiness for both day and night, the cloud heights in the Southern Hemisphere should be 2 to 4 km higher at night than in the daytime, and lower by 1 to 3 km in the Northern Hemisphere.

Similar analysis of the TIROS radiation data can also be made to determine the longitudinal as well as latitudinal distribution of nighttime cloud cover, but it requires more detailed information on the global distribution of surface temperatures, water vapor, and variations in the emissivities of land areas (Beuttner and Kern, 1963).

Acknowledgment. I wish to thank Professor R. M. Goody for reading over the manuscript and making valuable comments, L. Umscheid for programming and computing on an IBM 7094 and A. Liebman for his valuable assistance during the preparation of this paper.

REFERENCES

Arking, A., 1964: The latitudinal distribution of cloud cover from TIROS photographs. *Science*, **143**, 569–572.

Bandeen, W. R., R. A. Hanel, J. Licht, R. A. Stampfl and W. G. Stroud, 1961: Infrared and reflected solar radiation measurements from the TIROS II meteorological satellite. *J. geophys. Res.*, **66**, 3169–3185.

Beuttner, K. J. K., and C. D. Kern, 1963: Infrared emissivity of the Sahara from TIROS data. *Science*, **142**, 671–672.

Davis, P., 1962: A re-examination of the heat budget of the troposphere and lower stratosphere. *Scientific Report No. 3*, Contract No. AF 19(604)–6146, Research Division, College of Engineering, New York University. (AD-267 984, OTS price $10.00.)

Haurwitz, B., and J. M. Austin, 1944: *Climatology*. New York, McGraw-Hill Book Co., Inc., 410 pp.

London, J., 1957: A study of the atmospheric heat balance. Final Report, Contract No. AF 19(122)–165, Research Division College of Engineering, New York University. (OTS No. PB 129551, m. $5.60, ph $16.80.)

Nordberg, W., W. R. Bandeen, B. J. Conrath, V. Kunde and I. Persano, 1962: Preliminary results of radiation measurements from the TIROS III meteorological satellite. *J. atmos. Sci.*, **19**, 20–30.

Prabhakara, C., and S. I. Rasool, 1963: Evaluation of TIROS infrared data. *Proc. First Internat. Symposium on Rocket and Satellite Meteor.*, Amsterdam, North-Holland Publishing Co., 234–246.

Shiffrin, K. S., 1961: Spectral properties of clouds. *Geofis. pura. appl.*, **48**, 129–137.

Wark, D. Q., G. Yamamoto and J. H. Lienesch, 1962: Methods of estimating infrared flux and surface temperature from meteorological satellites. *J. atmos. Sci.*, **19**, 369–384.